Contributed paper

OPTO-ELECTRONICS REVIEW 8(2), 181–187 (2000)

Polarimetric sensors for weigh-in motion of road vehicles

P. WIERZBA* and B.B. KOSMOWSKI

Technical University of Gdańsk, Faculty of Electronics Telecommunication and Informatics, Department of Optoelectronics
11 Narutowicza Str., 80-952 Gdańsk, Poland

Weigh-in-motion (WIM) of road vehicles is a technology used in many applications, ranging from research to law enforcement. Sensors for WIM systems should exhibit high dynamic range, good accuracy and repeatability, as well as long service life. One of the most promising group of sensors for this application are polarimetric sensors, due to their simplicity and high sensitivity. Their viability for this application has been successfully demonstrated. Preliminary tests shown however, that the construction of the sensors should be modified to eliminate hysteresis and sensor's nonlinearity.

Keywords: polarimetric fibre sensor, weight-in-motion.

1. Introduction

The need for weighing road vehicles, which has been present for a long time in several applications, resulted in the development of several weighing techniques. These methods were based either on traditional weighing scale technology, or on strain gauges. The number of applications was severely restricted because the weighed vehicles were not allowed to move.

In the late sixties the development of new measurement methods made possible systems that can weigh a slowly moving vehicle, or can estimate the static weight of a vehicle travelling at a normal highway speed. These methods are referred to as low-speed weigh-in-motion (LS-WIM) and high-speed weigh-in-motion (HS-WIM), respectively. While LS-WIM is an established, mature technology, employing equipment similar to that used for static weighing, HS-WIM is a developing technology having substantial growth potential and much wider application range comparing to static and low speed weighing.

Currently, the applications of weigh-in-motion technology can be divided into five main groups: weight enforcement (i.e., detecting overloaded vehicles and subjecting their operators to an appropriate legal action), toll collection, maintenance planning and statistics, research (pavement degradation studies, suspension evaluation) and safety-related applications.

The majority of high-speed weigh-in-motion systems use bending plates, load cells [1], piezoelectric [2] or quartz sensors [3] as well as capacitive sensors to measure instantaneous axle load. Apart from them, two inductive loops are used per monitored lane, to determine the speed of vehicles passing over the sensor, based on the time needed to cover the distance between the loops.

A typical weigh-in-motion system, presented in Fig. 1, consists of sensors installed in pavement, detecting passing vehicles and providing information about the axle load. The sensors are connected to a signal conditioning circuit, which performs operations, like amplification, filtering, and analogue to digital conversion. Resulting stream of digital data is processed by a microcontroller assisted sometimes by a digital signal processor, yielding information about vehicle speed, distances between the axles and axle loads. Based on this information vehicles are classified into several groups (car, bus, truck, etc.), according to one of existing classification schemes, introduced by system manufacturers or defined in national or international standards, e.g., EUR 13, OECD, US FHWA 13, and FHWA 15. Subsequently, the information about vehicle class, weight, speed, date and time of recording is stored in system memory, either as a separate data record for each vehicle or in a statistical form (the number of vehicles per class in certain time).

In most of systems, gathered information is transmitted, at regular intervals, either by a dedicated link or by phone or radio modems to the user of the system. The rest of WIM systems, especially those installed for temporary measurements, rely on periodic data collection by a portable computer connected directly to them.

High-speed weigh-in-motion systems cannot be used for legal and commercial purposes, such as weight enforcement or cargo weighing due to their low accuracy and poor repeatability. The accuracy of weight estimation by these systems is between 5% and 30% in most cases. This is much worse than static or low-speed weighing systems, which typically have accuracy better than 0.05% or 100 kg.

*e-mail: pwierzba@pg.gda.pl

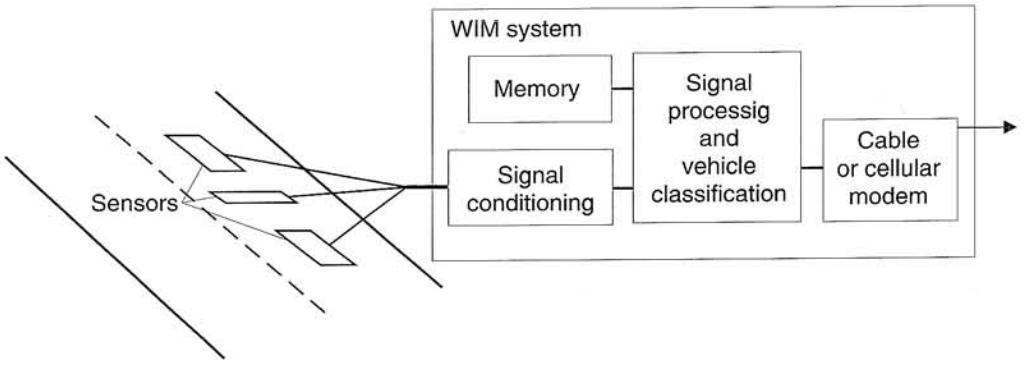

Fig. 1. Typical weigh-in-motion system.

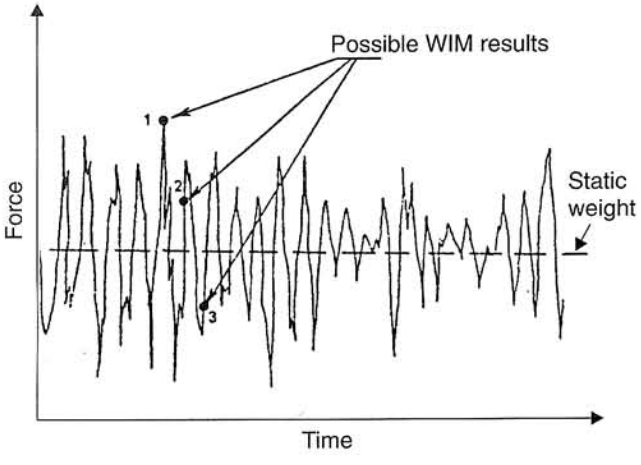

Fig. 2. Tyre force history and possible results of weighing in motion.

Such a low accuracy is caused mainly by the fact, that the static weight of a vehicle is estimated using only one or two measurements of instantaneous axle load. The axle load can contain a dynamic component of value up to 30–50% of static axle load, as shown in Fig. 2. Therefore, for a measurement taken using one or two sensors, the static weight estimate can differ from the static weight by a considerable amount. Because there is no repeatability in change patterns of dynamic component of axle load, the system cannot be calibrated to take this unwanted phenomenon into account. The accuracy can only be improved by using several sensors per monitored lane, along with effective data processing algorithms, which increases the system cost.

Most of sensors used by HS-WIM systems are installed flush with the pavement [1] or in slots made in the pavement and filled with epoxy [2], rather than directly in the pavement material. This creates surface inhomogenity, which may give rise to additional dynamic loading, leading to further accuracy deterioration. Unfortunately, because of low sensitivity these sensors cannot be embedded in the pavement.

To eliminate these shortcomings intense research is being conducted around the world, to design cost-effective multi-sensor HS-WIM systems and sensors. This effort has already resulted in development of interesting sensor constructions, such as piezoelectric quartz sensor. Other constructions are being investigated, most of them being optical fibre sensors.

Optical fibre sensors can offer important advantages in high-speed weigh-in-motion of road vehicles. Their intrinsic immunity to electromagnetic interference (EMI) allows them to be deployed in places where high EMI levels exclude the use of any electrical sensors. Unlike strain-gauge systems, optical fibre sensors do not require lightening protection, and are virtually free from interchannel crosstalk; therefore, a simpler detection and signal processing electronics can be used. The high sensitivity of optical fibre sensors (esp. interferometric and polarimetric) makes them a good choice for embedded applications where weak signals have to be measured.

Presently, the research is conducted on sensors using Mach-Zender or Fabry-Perot interferometers [4,5], microbending sensors [6] and polarimetric sensors [7]. The most promising of the sensors are the last two. Also the research on them is most advanced.

2. Principle of polarimetric sensor operation

When a section of polarisation maintaining (PM) fibre is subjected to transverse loading, two phenomena occur, namely polarisation mode coupling [8], and birefringence change [9]. The use of both phenomena for strain sensing has been demonstrated in Refs. 10 and 7, respectively. Because polarimetric sensors using mode coupling require an expensive tunable laser source or a sophisticated detection setup [11], they are not considered a viable choice for weigh-in-motion systems. Therefore, our further discussion will be limited to polarimetric sensors using stress-induced birefringence change.

Let us consider a polarimetric sensor presented in Fig. 3. The operation of sensor is following: the light from a laser diode is polarised by a polarising beam splitter and launched into a high birefringence transmission fibre, in such way, that only one polarisation mode is excited. Therefore, Jones vector describing the light is

$$\begin{bmatrix} E_x e^{j\omega t} \\ 0 \end{bmatrix}, \tag{1}$$

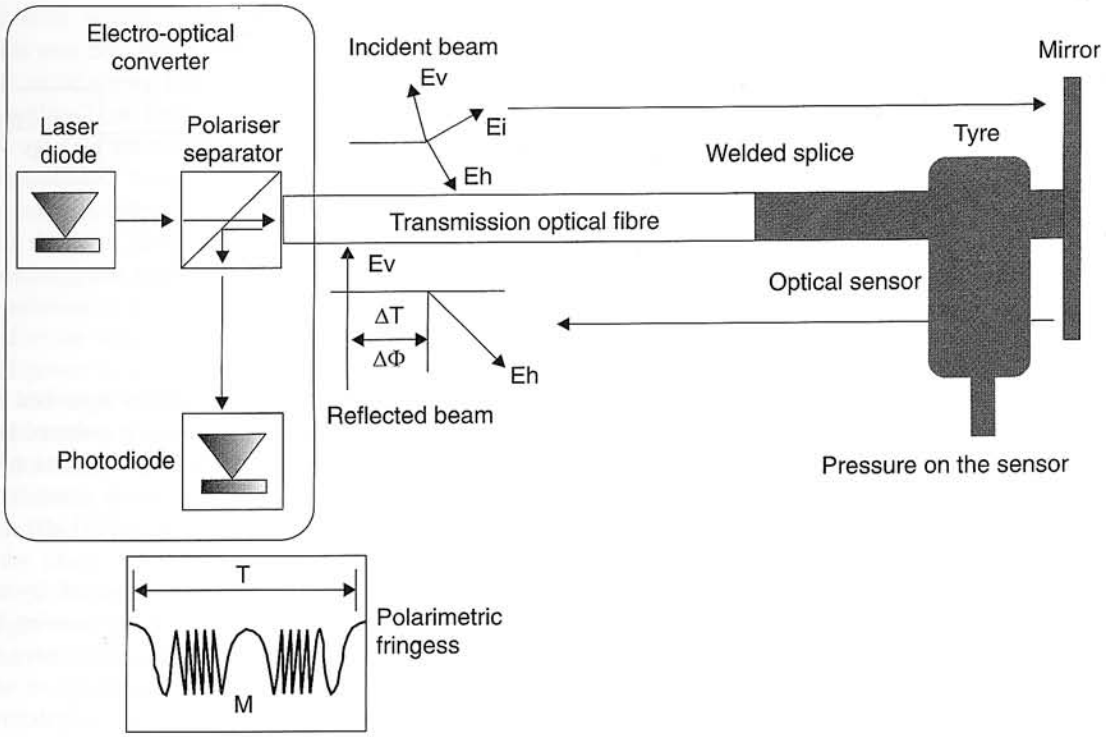

Fig. 3. Polarimetric force sensor.

and in normalised form

$$\begin{bmatrix} 1 \\ 0 \end{bmatrix}. \tag{2}$$

This mode propagates in the transmission fibre unchanged to the sensing fibre. On exiting the transmission fibre, the optical power is split equally between two polarisation modes of the sensing fibre (usually also high birefringence). It is achieved by aligning and splicing the sensing and transmission fibres in such a way, that their respective polarisation axes make an angle of 45°. Thus, normalised Jones vector corresponding to this situation is

$$\frac{1}{\sqrt{2}}\begin{bmatrix} 1 \\ 1 \end{bmatrix}, \tag{3}$$

Polarisation modes travel along the sensing fibre, are reflected from the mirror, and travel back to the transmission fibre. Because effective refractive indices are different for each polarisation mode, the modes propagate with different velocities v_1, v_2

$$v_1 = \frac{c}{n_{eff1}}; \quad v_2 = \frac{c}{n_{eff2}}, \tag{4}$$

where n_{eff1}, n_{eff2} are the effective refractive indices of respective modes, c is the speed of light in vacuum. The difference in propagating velocities of both modes gives rise to the phase delay between them. The phase difference between polarisation modes at the fibre's end can be expressed as

$$\varphi = 2\pi \frac{\Delta n_{eff}\, 2l}{\lambda}, \tag{5}$$

where l is the sensing fibre length, λ is the wavelength in vacuum, Δn_{eff} is the effective refractive index difference in sensing fibre. As effective refractive index difference Δn_{eff} in a single mode polarisation maintaining fibres is a function of temperature and stress applied to the fibre it is possible to measure force acting on the fibre by measuring the change of phase difference between polarisation modes.

Normalised Jones vector describing light emerging from the sensing fibre equals

$$\frac{1}{\sqrt{2}}\begin{bmatrix} 1 \\ e^{-j\varphi} \end{bmatrix}. \tag{6}$$

From the sensing fibre light propagates in the transmission fibre back to the beamsplitter. It can be shown that the light reaching the beamsplitter is described by a normalised Jones vector

$$\frac{1}{2}\begin{bmatrix} 1-e^{-j\varphi} \\ (1+e^{-j\varphi})e^{-j\Phi} \end{bmatrix}, \tag{7}$$

where Φ is the phase difference between polarisation modes introduced by the transmission fibre, given by

$$\Phi = 2\pi \frac{\Delta n_{eff}\, z}{\lambda}, \tag{8}$$

where z is the length of transmission fibre, λ is the wavelength in vacuum, Δn_{eff} is the effective refractive index difference in transmission fibre.

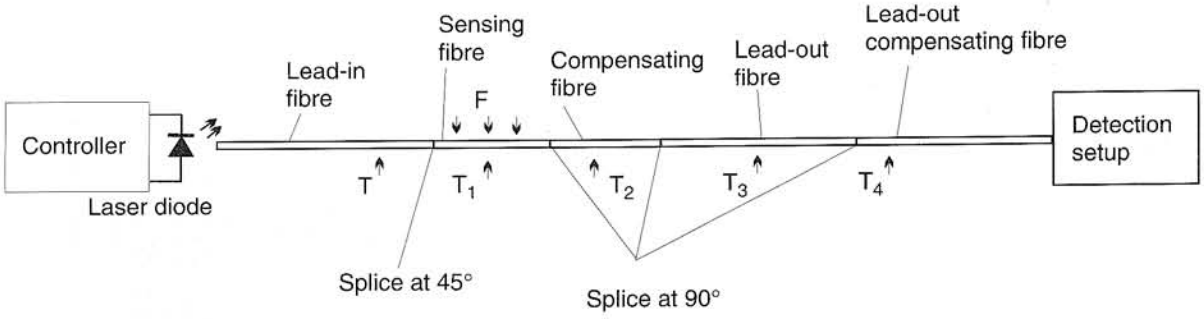

Fig. 4. Temperature compensated polarimetric sensor.

After passing polarising beamsplitter light intensity can be expressed as

$$I(\varphi) = I_0(1 + \cos(\varphi)), \tag{9}$$

where I_0 is the maximum light intensity. Knowing I_0 and measuring $I(\varphi)$ it is possible to calculate φ.

The advantage of configuration presented in Fig. 3 is that it allows for one-ended operation of the sensor. Apart from it, this configuration exhibits a few important disadvantages.

Firstly, the sensor is not temperature compensated, which means that temperature variations cause drift of the sensor signal. The amount of temperature-induced phase change ΔR is proportional to the total fibre length Z ($Z = z + l$) and temperature change ΔT. For a typical polarisation maintaining (PM) fibre (beat length 2 mm) it is equal

$$\frac{\Delta R}{Z\Delta T} = \pi \frac{rad}{m°C}, \tag{10}$$

i.e., one fringe per metre of fibre, per degree. For short fibres it is usually possible to filter out the drift, taking advantage from the fact that it is slow in comparison with strain changes caused by weighed vehicles. For longer fibres, it is either no longer possible, or it can introduce errors in weighing slowly moving vehicles.

Secondly, the examination of formula (9) shows that the direction of change of stress applied to the sensor cannot be determined based only on the intensity variations measurements, because of direction ambiguity for $\varphi = n\pi$. The sensor is also sensitive to intensity variations, which are measured as phase changes. This narrows its application areas to the measurements where the stress induced phase change is large enough (tens of radians or more) for fringe counting to be used.

Finally, the phase difference introduced by the transmission fibre requires the use of a light source with long coherence length. For a ten-metre high-birefringence fibre (beat length 2 mm) the coherence length should be more than 10 mm, which requires the use of a laser having linewidth of less than 0.1 nm. This means that an expensive distributed feedback (DFB) laser diode, rather than inexpensive Fabry-Perot (FP) laser diode, has to be used.

A sensor free from the drawbacks described above can be build by leveraging the experience gathered in the field of polarimetric pressure sensors [12]. The sensor, presented in Fig. 4, works in transmission mode using temperature compensation technique described in [13] and a detection setup shown in Fig. 5.

Temperature compensation is achieved by using two compensating fibre segments; one for sensing fibre, another for lead-out fibre. These segments have the same lengths as fibre segments they compensate, to which they are spliced fibres in such way, that their respective polarisation axes make an angle of 90°. This means that the modes are interchanged, i.e., the fast mode in first fibre becomes slow in the second and the slow mode in first fibre becomes fast in the second. In practice it is impossible to obtain two equal lengths of optical fibre. This gives rise to phase difference

$$\Delta\varphi = \frac{2\pi}{\lambda}\left(\Delta n_{eff1} l_1 - \Delta n_{eff2} l_2\right), \tag{11}$$

where λ is the wavelength in vacuum, Δn_{eff1} is the effective refractive index difference in sensing fibre, l_1 is the length of sensing fibre, Δn_{eff2} is the effective refractive index difference in compensating fibre, l_2 is the length of compensating fibre. Similar formula can also be written for lead-out and lead-out compensating fibre.

As long as the mean temperatures of respective fibres are equal, i.e., $T_1 = T_2$ and $T_3 = T_4$ (Fig. 4) and corresponding fibre lengths are matched to within 1%, temperature induced drift in the sensor is two orders of magnitude smaller than without compensation.

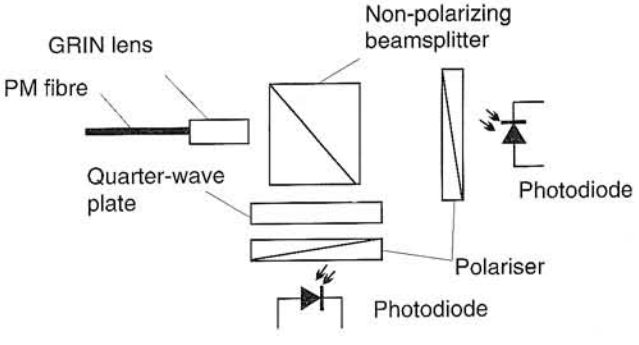

Fig. 5. Two-channel detection setup.

Apart from temperature compensation, this arrangement yields near zero phase difference for both polarisation modes. It can be shown that if the fibre dimensions are accurate to within 2 cm, the laser linewidth can be as wide as 5 nm, allowing for the use of inexpensive laser diodes.

The operation of transmissive temperature compensated sensor is similar to already described reflective sensor. The light from the laser diode is polarised and launched into a high birefringence transmission fibre, in such way, that only one polarisation mode is excited. This mode propagates unchanged to the sensor. On exiting the transmission fibre, the optical power is split equally between two polarisation modes of the high birefringence sensing fibre by a 45° splice. Polarisation modes travel with different velocities through the sensing fibre, compensating fibre, lead-out fibre and lead-out compensating fibre, which are connected by 90° splices. The stress applied to the sensing fibre segment changes the phase delay between the polarisation modes, which in turn changes the state of polarisation of the light.

The light emerging from the lead-out compensating fibre is described by normalised Jones vector

$$\frac{1}{\sqrt{2}}\begin{bmatrix}1\\ e^{-j(\Delta\varphi_1+\Delta\varphi_2+\delta)}\end{bmatrix}=\frac{1}{\sqrt{2}}\begin{bmatrix}1\\ e^{-j\varphi}\end{bmatrix}, \tag{12}$$

where $\Delta\varphi_1$ is the phase difference caused by length mismatch of sensing and compensating fibre segments, $\Delta\varphi_2$ is the phase difference due to the length mismatch of lead-out and lead-out compensating fibre segments, δ is the stress induced phase difference.

The detection setup, shown in Fig. 5, produces two signals

$$\begin{aligned} U_1 &= I_0(1+\cos\varphi),\\ U_2 &= I_0(1\mp\sin\varphi). \end{aligned} \tag{13}$$

The phase difference of these signals is 90°; therefore it is always possible to determine the direction of applied stress changes. Total power of the light exiting the fibre also can be determined from Eq. (13), making sensor insensitive to received power fluctuations.

If a pigtailed laser is used, the mechanical construction of the sensor is also simplified, as there is no need for precision alignment of laser, beamsplitter and the fibre.

However, parameters of the sensor described above are not completely independent of temperature because of a second-order effect of temperature on sensitivity [14,15]. Fortunately the change caused by it is relatively small. This effect can be further reduced by using a special PM fibre, having their properties optimised by the proper choice of materials [16].

3. Measurements

The sensor presented in Fig. 3 and using a modulator from Fig. 6 was subjected to static tests in order to verify its linearity and measurement range as well as determine dependence of these parameters on metallic ribbon geometry [9]. These tests were conducted using sensors without temperature compensation. Sensor response as a function of applied load was measured for modulators made using ribbons of different thickness and width. Example results of these measurements are presented in Fig. 7 [7], showing considerable nonlinearity. Similar static measurements, made using a sensor embedded in polyurethane, and narrower range of loads [7], resulted in linear characteristics, but significant hysteresis. The amount of hysteresis is so big that it restricts the operation of such sensor to fringe-counting regime. This hysteresis can be caused either by cladding exhibiting inelastic behaviour or arise in the modulator construction. To pinpoint the exact reason we made an experiment using a modulator consisting of two stiff aluminium disks, with the fibre under test placed between them, and a simple loading setup. The disks were entirely separated by the fibre; careful alignment guaranteed that no shearing stress was applied to the fibre. The re-

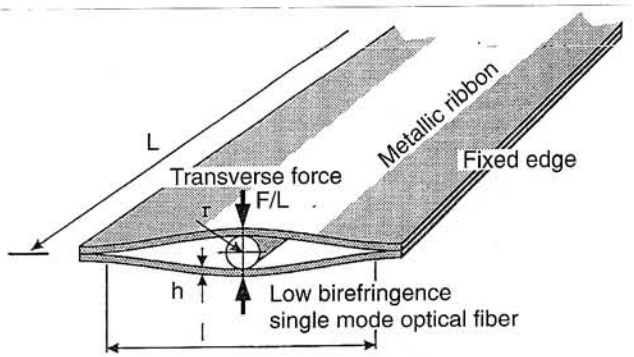

Fig. 6. Modular detail.

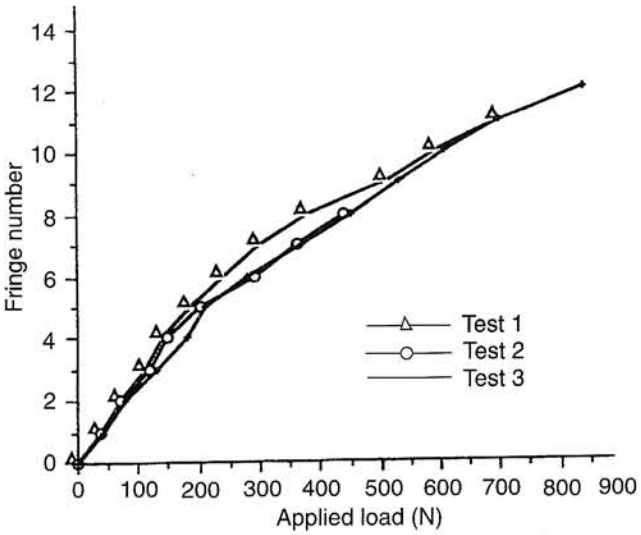

Fig. 7. Sensitivity of a polarimetric sensor using modulator shown in Fig. 6. Three subsequent tests of the same modulator are presented.

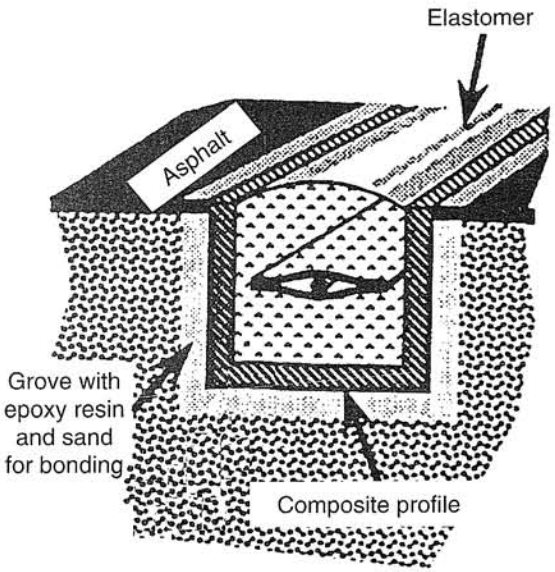

Fig. 8. Polarimetric sensor for weigh-in motion of road vehicles.

sults obtained in these measurements [17] are in good agreement with those presented previously.

Dynamic measurements of the sensor presented in Fig. 3 and using a modulator shown in Fig. 6 were performed in normal road conditions [7] using a compact car as a testing vehicle. The sensor was installed in the road using a composite profile mounted flush with the road surface and filled with polyurethane. Installation details are presented in Fig. 8. Detection setup operated in fringe counting mode using a simple algorithm to recover phase change. Several measurements were carried out showing fairly good repeatability.

4. Discussion

Measurement results presented above show significant sensor hysteresis and nonlinearity. Both these phenomena seriously affect sensor performance. Therefore, further research is needed to make possible the use of polarimetric sensors for weigh-in-motion applications.

The analysis of possible hysteresis sources, and results presented in Fig. 7, show that the drift is most likely caused by properties of cladding, which exhibit inelastic behaviour. This can be overcome by using different cladding materials (so-called hard cladding, i.e., made from diamond, certain metals, or silicon nitride). Currently, polarisation maintaining fibres with such cladding are not available because of technological and economic reasons. Hard cladding can only be applied during a fibre draw process, which requires not only serious modifications to the fibre draw equipment, but it also uses techniques foreign to optical fibre industry. Because the need for such cladding arises in several applications, we hope that such fibres will be available in the not too distant future.

Nonlinearity of the sensor is caused by the fact, that with increasing force acting on it, the contact area of ribbons increases. As a result, greater part of total stress is applied to the ribbon contact areas, rather than to the sensing fibre, decreasing sensitivity.

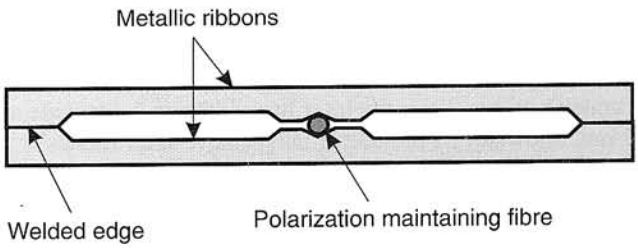

Fig. 9. Improved modular design.

This source of error can be fairly easily eliminated, using a modulator design with clearly defined ribbon contact area, as shown in Fig. 9.

5. Conclusions

Experiments with polarimetric optical fibre sensors have demonstrated their suitability for weigh-in-motion applications. Preliminary tests indicate that the performance of these sensors is affected by nonlinearity and hysteresis. Therefore, the construction of the sensors should be modified in order to eliminate the unwanted phenomena.

The compensation scheme using two compensating fibre segments presented in the article not only eliminates first-order temperature-induced drift, but it allows inexpensive laser diodes to be used, leading to a substantial sensor cost reduction.

References

1. B. McCall and W.C. Vodrazka, Jr., *State's Successful Practices Weigh-In-Motion Handbook*, Department of Transportation, Federal Highway Administration, available from: http://www.ctre.iastate.edu/projects/attech/WIM-pdf/.
2. G. Bailleul, *Vibracoax Ceramic Piezoelectric Traffic Sensors*, available from: http://www.nmsu.edu/~traffic/NATDAC96/bailleul.htm.
3. R. Calderara, "Long-term stable quartz WIM sensor", *National Data Acquisition Conference*, Albuquerque, New Mexico, USA, 1996.
4. S. Meller, N. Zabaronik, I. Ghoreishian, J. Allison, V. Arya, M.J. de Vries, and R.O. Claus, "Performance of fibre optic vehicle sensors for highway axle detection;" *Proc. SPIE* **2902**, 168–175 (1997).
5. S. Meller, M.J. de Vries, V. Arya, R.O. Claus, and N. Zabaronik, "Advances in optical fibre sensors for vehicle detection", *Proc. SPIE* **3207**, 318–322 (1998).
6. P. Suopajärvi, R. Pennala, M. Heikkinen, P. Karioja, V. Lyöri, R. Myllylä, S. Nissila, H. Kopola, and H. Suni, "Fiber optic sensors for traffic monitoring applications", *Proc. SPIE* **3325**, 222–229 (1998).
7. S.R. Teral, S.J. Larcher, J.M. Caussignac, and M. Barbachi, "Fiber optic weigh-in-motion sensor: correlation between modelling and practical characterisation", *Proc. SPIE* **2718**, 417–426 (1996).

8. M. Tsubokawa, T. Higashi, and Y. Negishi, "Mode coupling due to external forces distributed along a polarisation-maintaining fibre: an evaluation", *Appl. Opt.* **27**, 166–173 (1988).
9. M. Barbachi and J.M. Caussignac, "Development of a single-mode optical fibre sensor for civil engineering applications", *Proc. SPIE* **2718**, 398–407 (1996).
10. S.V. Miridonov, M.G. Shlyagin, A.V. Khomenko, and D. Tentori, "Distributed polarimetric fibre-optic sensors using wavelength-scanning technique", *Proc. SPIE* **3094**, 194–203 (1997).
11. A. Mazikowski, H.J. Wierzba, and P. Wierzba, "Distributed polarimetric optical fibre strain sensor using a tunable laser source", *Proc. SPIE* **3730**, 27–31 (1999).
12. W.J. Bock and W. Urbańczyk, "Temperature desensitisation of a fibre-optic pressure sensor by simultaneous measurement of pressure and temperature", *Appl. Opt.* **37**, 3897–3901 (1998).
13. J.P. Dakin and C.A. Wade, "Compensated polarimetric sensor using polarisation maintaining fibre in differential configuration", *Electr. Lett.* **20**, 51–53 (1984).
14. J. Ma and W. Tang, "Second-order sensitivity effects on optical fibre polarimetric temperature sensor and strain sensor", *Appl. Opt.* **36**, 9010–9013 (1997).
15. W.J. Bock and W. Urbańczyk, "Temperature-hydrostatic pressure cross-sensitivity effect in elliptical-core, highly birefringent fibres", *Appl. Opt.* **35**, 6267–6270 (1996).
16. J. Wójcik, B. Janoszczyk, M. Makara, K. Poturaj, W. Spytek, A. Walewski, W. Urbańczyk, and W.J. Bock, "Experimental investigation of the effect of protective coatings on temperature sensitivity of side-hole optical fibres", *Proc. SPIE* **3189**, 38–43 (1997).
17. B.B. Kosmowski, A. Mazikowski, and P. Wierzba, "Polarimetric optical fibre strain sensor", *Proc. SPIE* **3730**, 22–26 (1999).